Highlights

1. Stochastic identification helps avoid finding unstable human postural controllers.
2. It tracked the experimental data nearly as well as deterministic identification.
3. Comparing to eigenvalue constraints, linearization is not needed in it.
4. It can be applied on highly nonlinear systems and large data-sets identifications.

Identification of the Human Postural Control System through Stochastic Trajectory Optimization

Huawei Wang and Antonie J. van den Bogert

h.wang59@vikes.csuohio.edu, a.vandenbogert@csuohio.edu
Mechanical Engineering
Washkewicz College of Engineering
Cleveland State University
2121 Euclid Avenue, Cleveland, OH 44115, USA

Abstract

Background: System identification can be used to obtain a model of the human postural control system from experimental data in which subjects are mechanically perturbed while standing. However, unstable controllers were sometimes found, which obviously do not explain human balance and cannot be applied in control of humanoid robots. Eigenvalue constraints can be used to avoid unstable controllers. However, this method is hard to apply to highly nonlinear systems and large identification datasets.

New method: To address these issues, we perform the system identification with a stochastic system model where process noise is modeled. The parameter identification is performed by simultaneous trajectory optimizations on multiple episodes that have different instances of the process noise.

Results: The stochastic and deterministic identification methods were tested on three types of controllers, including both linear and nonlinear controller

architectures. Stochastic identification tracked the experimental data nearly as well as the deterministic identification, while avoiding the unstable controllers that were found with a deterministic system model.

Comparison with Existing Method: Comparing to eigenvalue constraints, stochastic identification has wider application potentials. Since linearization is not needed in the stochastic identification, it is applicable to highly nonlinear systems, and it can be applied on large data-sets.

Conclusions: Stochastic identification can be used to avoid unstable controllers in human postural control identification.

Keywords: Human standing balance, indirect identification, feedback controller, stability, stochastic environment

---

1. Introduction

Feedback control is a well accepted paradigm for human postural balance (Kuo, 1995). Identification of a feedback control system from human experiments has several important applications. In neuroscience, control system models are used to understand how humans maintain balance. In clinical applications, a quantitative description of the control system, e.g. as feedback gains and time delays, may have clinical applications. Finally, in humanoid robotics, a control system identified from human subjects can produce behavior that is more human-like than a control system designed from conventional control engineering principles.

System identification methods have been used, in both frequency and time domains, to identify feedback controllers from human experiments (Peterka, 2002; Park et al., 2004; Van Der Kooij and De Vlugt, 2007). In the frequency domain, information of human neuromuscular control were identified on experimental data with multiple random perturbations (Peterka, 2002; Van Der Kooij and De Vlugt, 2007; Boonstra et al., 2013; Kiemel et al., 2011; Engelhart et al., 2016; Afschrift et al., 2016). In the time domain, parametric controllers were usually identified and it has been shown that one perturbation is sufficient for multiple-input multiple-output (MIMO) system identification (Goodworth and Peterka, 2018). For instance, full-state proportional-derivative (FPD) controllers were identified on short experimental data where ramp perturbations were applied to the standing surface. Results showed that controller gains were proportional to the amplitudes of ramp perturbations (Park et al., 2004; Welch and Ting, 2009), which sug-

gests a nonlinear control system.

However, one common issue of the time domain identification work is that the best fit to the experiment was sometimes achieved with a controller that causes the closed loop system to be unstable. (Park et al., 2004; Goodworth and Peterka, 2018). While the best fit controller is always treated as the best identified controller, it is not useful since it can neither be applied to humanoid robots nor explain how humans control themselves. One possible reason of finding unstable controllers is that the process noise in both human system and experiment is not modeled. The identified controllers may take advantage of instability and sensitivity to initial conditions to achieve the best fit without falling.

To avoid instability, eigenvalue constraints have been used in the controller identification. It enforces eigenvalues of the modeled closed loop system to be negative at a specific pose while identifying the controller parameters. This method was successful in avoiding unstable linear controllers in standing balance identification under ramp perturbations (Park et al., 2004). However, the application of this method is limited. For instance, it cannot work with highly nonlinear systems, since only a limited set of linearization points can be checked. For complex tasks such as walking, this could become impractical. In addition, it is hard to incorporate eigenvalue constraints into identifications with long experimental recordings, in which gradient-based optimization and collocation methods are needed. Long recordings, under continuous random perturbation, are needed to collect sufficient informa-

tion to identifying more complex posture controllers. Direct collocation has been reported to be more efficient in such parameter identification problems (Kelly, 2017; Moore and van den Bogert, 2018).

In this paper, we hypothesize that a stochastic optimization, in which process noise is modeled, can help avoid finding unstable controllers in the standing balance identification problem. The stochastic optimization was applied on the identification of three types of controllers. Eigenvalue and forward simulations tests were done to examine the stability of the identified systems.

2. Method

An indirect identification approach was used in this study (Peterka, 2002; Park et al., 2004; Van Der Kooij and De Vlugt, 2007; Goodworth and Peterka, 2018). In the indirect approach, a model is built, which mathematically represents the closed loop system and an optimization method is used to fit experiment data by optimizing the model parameters. It has been reported that, in identifying the feedback controllers, the indirect approach can avoid the bias introduced by the direct approach which only uses the information of controller input and output (van der Kooij et al., 2005). In this paper, the mathematical model of the human standing balance system was treated as a closed-loop system which includes a body dynamics model and a feedback controller. The body dynamics model was simplified as a double-link pendulum, since ankle and hip strategies are mostly used for standing balance (Horak and Nashner, 1986). Three feedback controllers, as described below, were identified. The goal of the identification is to find the feedback

controller parameters P which enable the closed-loop system generate the response that is closest to the human experimental data (Fig. 1).

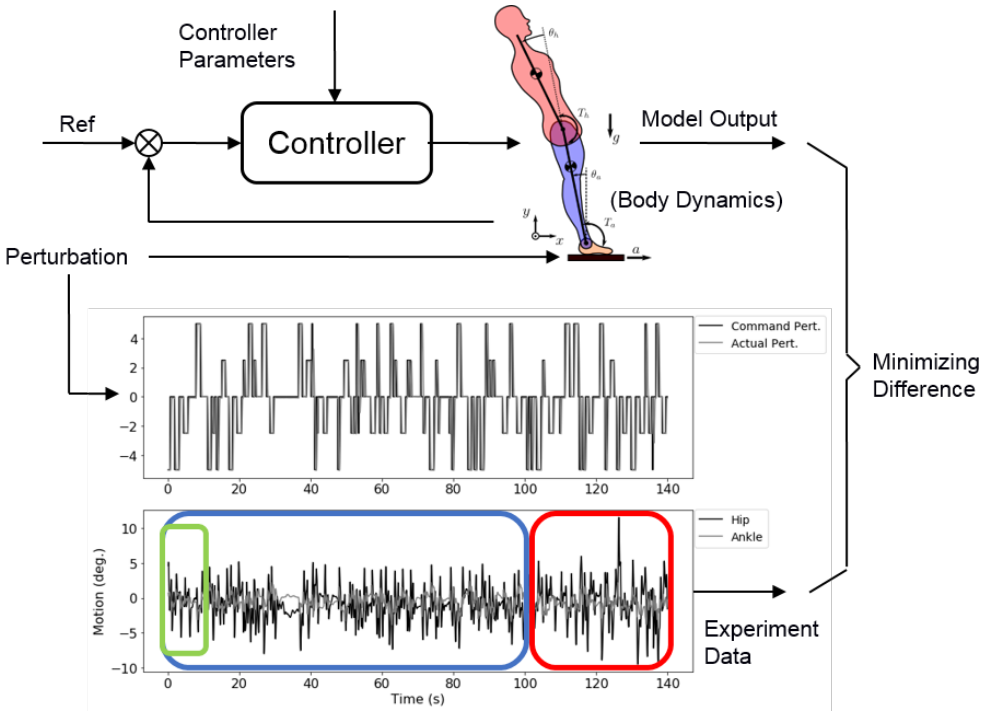

Figure 1: For identification of controller parameters, the same perturbation which was applied in the experiment was applied to the closed-loop system model. Controller parameters are optimized to fit the experimental data. The experimental data (140 seconds) was divided into 3 sections. The first 100 seconds (blue) were used to identify the linear controllers. The first 10 seconds (green) were used to identify the nonlinear controller. The last 40 seconds (red) were used to verify all identified controllers.

2.1. Experiments

Experiments were performed on six participants (five male, one female, age 18-34 years) with approval from the Institutional Review Board of Cleveland State University with the study number IRB-FY2018-40. A R-Mill in-

strumented treadmill (Forcelink, Netherlands) was used to induce anterior-posterior (AP) perturbations of the standing platform through its "sway" mechanism. Participants were asked to stand with their arms crossed in front of their chest and instructed to keep balance without taking a step. The perturbation signal was designed using random square pulses with five amplitudes ([-5, -2.5, 0, 2.5, 5] cm), and six pulse durations ([0.25, 0.5, 0.75, 1.0, 1.25, 1.5] seconds). Amplitudes and durations were randomly selected to generate a 140 second perturbation signal. Twenty-seven reflective markers were placed on each participant to record their reactions using a 10-camera motion capture system (Osprey 00882967, Motion Analysis Corp. Santa Rosa, CA). Hip and ankle joint motions were calculated from the recorded marker data, and the platform motion was recorded from encoders. The commanded perturbation signal, actual perturbation signal (standing platform motion) and balance reaction data (ankle and hip motion) of one participant can be found in Fig. 1. Data from one participant was used to show how the modeling of a stochastic environment affects the stability of identified controllers.

2.2. Controller Structures

Three feedback controllers were identified on the data described in Section A. Two of them are linear: a proportional-derivative (PD) controller and a full-state proportional-derivative (FPD) controller. The other one is nonlinear: neural network (NN) controller. Formulas of these three controllers are shown below:

PD controller:

$$\begin{bmatrix} T_a \\ T_h \end{bmatrix} = \begin{bmatrix} K_{p_a} & 0 & K_{d_a} & 0 \\ 0 & K_{p_h} & 0 & K_{d_h} \end{bmatrix} \begin{bmatrix} \theta_a - \theta_a^r \\ \theta_h - \theta_h^r \\ \dot{\theta}_a \\ \dot{\theta}_h \end{bmatrix} \tag{1}$$

FPD controller:

$$\begin{bmatrix} T_a \\ T_h \end{bmatrix} = \begin{bmatrix} K_{p_{aa}} & K_{p_{ah}} & K_{d_{aa}} & K_{d_{ah}} \\ K_{p_{ha}} & K_{p_{hh}} & K_{d_{ha}} & K_{d_{hh}} \end{bmatrix} \begin{bmatrix} \theta_a - \theta_a^r \\ \theta_h - \theta_h^r \\ \dot{\theta}_a \\ \dot{\theta}_h \end{bmatrix} \tag{2}$$

where T_a and T_h are ankle and hip joint torques; θ_a and θ_h are ankle and hip joint angles; θ_a^r and θ_h^r are the reference joint angles for ankle and hip at quiet standing; $\dot{\theta}_a$ and $\dot{\theta}_h$ are ankle and hip joints angular velocities; K_p and K_d are proportional and derivative gains of feedback controllers.

For the nonlinear controller, a standard neural network architecture (Jain et al., 1996) with 1 hidden layer and 4 hidden nodes was used. The inputs are the system state and a constant value node, and the outputs are joint torques. The smoothed leaky-ReLU function was used as activation function and is showing in Equation .3. The reason to smooth the activation function is make it continuously differentiable, which is essential to gradient-based optimization.

$$f(x) = x + 0.7(\frac{x - \sqrt{x^2 + 0.0001}}{2}) \tag{3}$$

The control parameters in the two types of linear controllers are the proportional-derivative gains K and reference joint angles θ^r. The control parameters in neural network are the weights W_{ij} applied in between the input layer, the hidden layer, and output layer. The total number of controller parameters in the PD, FPD, and NN controllers are 6, 10 and 30, respectively.

2.3. Controller Identification in Deterministic Environment

Deterministic environment, without modeling of process noise, has been used in most controller identification studies (Park et al., 2004; Van Der Kooij and De Vlugt, 2007; Goodworth and Peterka, 2018). The deterministic standing balance controller identification problem was defined as a combined trajectory and parameter optimization problem:

$$\begin{aligned} &\text{Optimize trajectory } x(t) \text{ and control parameters } P \\ &\text{Minimize objective function } F = \int_0^T \|\theta_m(t) - \theta(t)\|^2 dt \\ &\text{Subject to: body dynamics: } f(x(t), \dot{x}(t), P, a) = 0 \end{aligned} \tag{4}$$

where $x(t)$ is the state trajectory of the identified system, including ankle/hip joint angles θ and angular velocities $\dot{\theta}$; P represents the control parameters inside the feedback controller; T is the total time period of the measured experimental data; θ_m is the measured joint angles; θ is the optimized joint angles; a represents the acceleration of perturbation;

2.4. Controller Identification in Stochastic Environment

In a stochastic environment, process noise is considered in the controller identification process. In controller identification with stochastic environ-

ment, the optimization is carried out over multiple episodes. Each episode simulates the motions with the same controller, and the same perturbation signal, but with a different process noise signal. The identification problem for the stochastic environment is defined below:

$$\begin{aligned}
&\text{Optimize trajectory } \{x^1(t), ..., x^M(t)\} \text{ and Controller Parameters } P \\
&\text{Minimize objective function: } F = \sum_{s=1}^{M} \left(\int_0^T \|\theta_m(t) - \theta^s(t)\|^2 * dt \right) \\
&\text{Subject to: body dynamics: } \left\{ \begin{array}{c} f_1(x(t), \dot{x}(t), P, a) + n_1(0, \sigma) = 0 \\ ..... \\ f_s(x(t), \dot{x}(t), P, a) + n_s(0, \sigma) = 0 \\ ..... \\ f_M(x(t), \dot{x}(t), P, a) + n_M(0, \sigma) = 0 \end{array} \right\}
\end{aligned} \tag{5}$$

where M is the total number of episodes; s is the s^{th} episode; $x^s(t)$ is the state trajectory of human system model in s^{th} episode; $n_s(0, \sigma)$ is random noise added to s^{th} episode.

The direct collocation method (Hargraves and Paris, 1987) was used in this paper. This transforms the trajectory optimization problem into nonlinear program (NLP) with a finite number of unknowns: the states x at N collocation nodes, and the controller parameters (Moore and van den Bogert, 2015, 2018). The Midpoint Euler approximation was used to convert the body dynamics constraint into algebraic constraints:

$$f(\frac{x_{i+1} + x_i}{2}, \frac{x_{i+1} - x_i}{h}, P, a) = 0, \quad for\ i = 1, 2, ..., N-1. \tag{6}$$

The number of collocation nodes was 50 per second, and IPOPT was used to solve the NLP (Wächter and Biegler, 2006).

Four identification problems were solved for each controller structure. For each controller, a deterministic identification was performed first. For the linear controllers (PD, FPD), stochastic identifications with 2, 3, and 4 episodes were performed. For the nonlinear neural network controller, stochastic identification were performed with 6, 8, and 10 episodes. The process noise was modeled as Gaussian random noise with amplitude of $\pm$ 0.25 Nm, added to the controller outputs (joint torques) at each time step. The process noise in each episode was randomly generated, and kept the same during the optimization process. For each identification problem, 10 optimizations with random initial guesses were performed. By selecting the best fit with experiment data among 10 optimizations, local optimum results can be largely prevented.

2.5. Stability evaluation

Eigenvalues and forward simulations were used to evaluate the stability of the closed loop standing balance system with the identified controllers. In the eigenvalue test, the closed loop system dynamics were linearized to obtain eigenvalues at different operating points. These points covered the range of motion observed in the experiment. In the forward simulation tests, the identified controllers were used to perform 40 seconds simulations with all possible initial conditions inside the experiment data range. The perturbation (in red block) used in the forward simulation was different from the perturbation used in identifications. No process noise was used in these tests.

The distribution of four state variables (ankle angle, hip angle, ankle angular velocity, hip angular velocity) in the experimental data is shown in figure 2A. Ranges of these four state variables in degree (degree/s) are between [-3.87, -9.49, -16.53, -50.74] and [2.41, 11.50, 18.38, 65.00]. To check the stability of identified controllers in a standard way, eleven equidistant values were chosen within the range of each state variable, resulting in $11 * 11 * 11 * 11 = 14641$ operating points where eigenvalues were calculated. The percentage of stable operating points (all eigenvalues negative) was calculated. Forward simulation tests used each of these operating points as an initial condition. A simulation was considered stable if the root mean square (RMS) between the forward simulations and the experiment data was within 3 times the standard deviation of experiment data. The percentage of stable simulations was calculated for each identified controller. The eigenvalue and forward simulation tests were performed using the Ohio Super Computer System (Center, 1987).

3. Results

Results of the identifications are summarized in Fig. 2. The percentage of stable eigenvalues and forward simulations (Fig. 2b) is always below 100%. One reason is that many of the checking points were outside of the range of actual state trajectories. Nevertheless, the effect of identification method on stability was clearly seen.

In the PD and NN controllers, results show that mostly stable controllers can

be found by introducing a stochastic environment, while unstable controllers were found in the deterministic identifications. When the stochastic environment was introduced and the episode number increased to a specific number (3 episodes for PD controller type, 8 episodes for NN controller type), stable controllers were found, which resulted in high percentages of stable eigenvalues and stable forward simulations.

In the FPD control architecture, the deterministic identification already produced stability in about half of the tests. With the stochastic environment (2, 3, and 4 episodes), the percentage of stable eigenvalues and forward simulation remained high.

4. Discussion

Our results confirmed previous findings of unstable controllers when a deterministic model is used for identification of the human postural control system (Park et al., 2004; Goodworth and Peterka, 2018). The optimization is likely taking advantage of instability to improve the fit. In a deterministic unstable system, the final state can be made equal to the corresponding measurement, by extremely small changes in initial condition or controller parameters. We hypothesized that with a stochastic model, the optimization can no longer take advantage of instability to improve the fit with the experiment. The stability tests using eigenvalue analysis and forward simulation tests supported our hypothesis. We also found that stochastic approach did not effect the stability very much when the deterministic approach already found a stable controller. Identified control gains and eigenvalue distributions of PD and

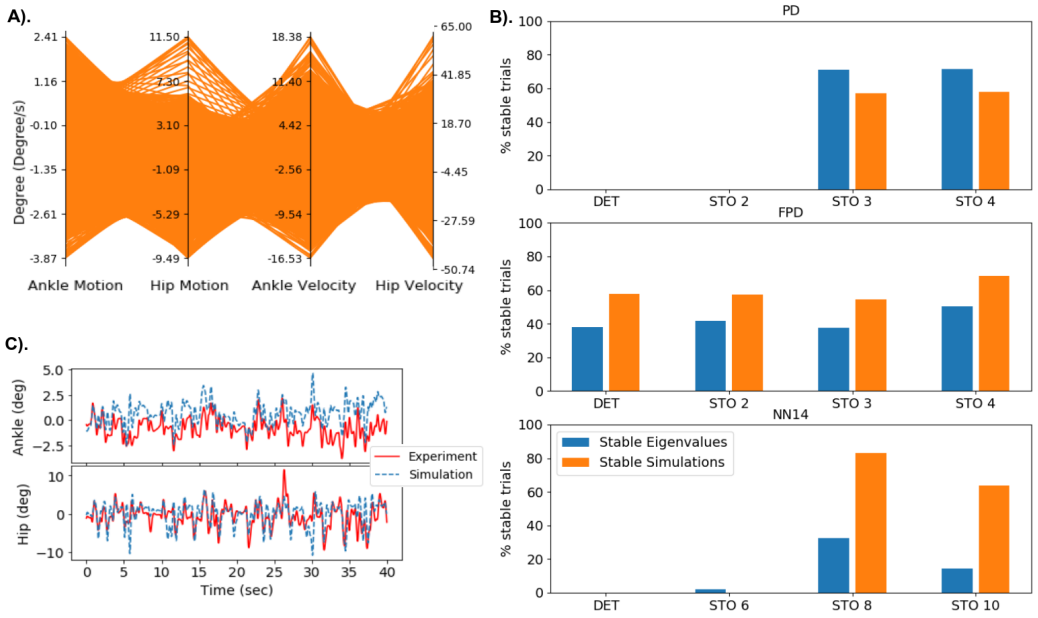

Figure 2: Eigenvalue and forward simulation test of identified best controllers among the whole state points. Subplot A is the range of each state variable from the human standing experiment data. subplot B is the percentages of stable eigenvalue and stable forward simulations of all 12 identified best controllers at all selected state points. "DET" means deterministic optimization. "STO i" means stochastic optimization with i episodes. Subplot C is one comparison between forward simulation and experiment data. RMS of this this forward simulation is about 1.3 STD of experiment data.

FPD controllers are shown in Appendix. In general, stable controllers identified from stochastic model are close to these unstable controllers identified through deterministic approach.

The eigenvalue analysis and forward simulation tests were mostly in agreement about the stability of the system, except in the NN controller. This is not surprising because linearization may not give a reliable evaluation of

stability in a system with strong nonlinearities. This finding also suggests that the use of eigenvalues as constraints in the identification problem (Park et al., 2004) is not likely to give useful results for nonlinear controllers. In contract, the stochastic trajectory optimization presented here is directly applicable to nonlinear systems without linearization.

Generally, more episodes were needed to find stable best controllers for more complex controllers with more free parameters. In the case of our study, identification of a stable PD controller requires three episodes, while identification of a stable NN controller required eight episodes to get stable controllers. Because controller parameters (which are the same in each episode) and free initial conditions (which are different in each episode) can both be used to take advantage of instability, we suspect that the required number of episodes equals the number of control parameters divided by the number of system state variables.

The amplitude of Gaussian noise used in this paper was 0.25 Nm, applied to the joint torques of human balance system. This is approximately one percentage of the standard deviation of the joint torques in the standing balance experiment. An amplitude of 0.5 Nm was also tried, which had the same stability effect of 0.25 Nm but resulted in slightly larger control parameter differences between the identified stable controllers.

Recently, similar ideas of using a stochastic environment were also used in other studies to get realistic and stable results in robotic control. Mordatch

increased the success rate of path planning in a biped robot by adding model uncertainty (Mordatch et al., 2015). Policies for robot arm control were obtained by reinforcement learning in a simulated stochastic environment, making them robust enough for transfer to hardware (Peng et al., 2018). Although these control optimization studies were not system identifications from experimental data, they share with our work the use of a simplified model of the real system. In order to avoid overly specialized controllers, stochastic dynamics can be used to produce better and more realistic solutions.

5. Conclusion

In this work, we showed that identification of human standing balance controllers by stochastic trajectory optimizations will produce controllers that are more robust than those obtained with a deterministic system model. When applied in robotic systems, these identified controllers will result in human-like behavior that is stable against small perturbations.

Acknowledgement

The authors would like to thank the National Science Foundation (grant No. 1344954) and the Ohio Supercomputer Center.

Conflict of interest

Declarations of interest: none

Appendix

1. Gains and eigenvalue distributions of identified controllers in both deterministic and stochastic environments.

Identified control gains of PD and FPD control structures are shown in Table 1 and 2. Weights of neural network controller is not shown here, since they do not have a realistic meaning. Eigenvalue distributions of the identified PD and FPD controllers are shown in Table 3 and 4. Eigenvalues are calculated at the neutral pose (standing straight) which is close to the close-loop system equilibrium point. Eigenvalue of neural network controllers are not shown either, since eigenvalue at one point does demonstrate stability for nonlinear systems. All proportional gains Kp shown blow have a unit of Nm/rad. All derivative gains Kd shown blow have a unit of $Nm * s/rad$. All reference angles Ref have a unit of rad. In the Table II (FPD controllers), foot xy after Kp and Kd means the signal transfer path from x to y. For instance, $Kp_{,ah}$ means a proportional gain that use the feedback information of hip to the control target of ankle. Experimental data, identification code, and related results were included in a public GitHub repository https://github.com/HuaweiWang/Stochastic_Paper.

Table 1: Identified control gains in the PD control structure

	DET	STO2	STO3	STO4
$Kp_{,ankle}$	883.80 ± 0.08	766.04 ± 0.00	972.25 ± 1.84	970.91 ± 1.52
$Kd_{,ankle}$	18.33 ± 0.01	20.33 ± 0.00	29.68 ± 1.25	30.23 ± 1.12
$Kp_{,hip}$	222.05 ± 0.01	224.24 ± 0.00	236.58 ± 0.57	236.94 ± 0.58
$Kd_{,hip}$	8.99 ± 0.00	7.84 ± 0.00	10.57 ± 0.03	10.56 ± 0.03
$Ref_{,ankle}$	0.0014 ± 0.00	0.0026 ± 0.00	0.0007 ± 0.00	0.0007 ± 0.00
$Ref_{,hip}$	-0.0005 ± 0.00	-0.0006 ± 0.00	-0.0015 ± 0.00	-0.0016 ± 0.00

Table 2: Identified control gains in the FPD control structure

	DET	STO2	STO3	STO4
$Kp_{,aa}$	341.49 ± 0.57	431.78 ± 5.17	454.75 ± 37.77	453.08 ± 34.30
$Kp_{,ah}$	412.23 ± 0.47	336.78 ± 4.23	318.62 ± 28.74	322.54 ± 27.21
$Kd_{,aa}$	68.84 ± 0.10	59.35 ± 0.85	55.29 ± 5.58	56.30 ± 4.86
$Kd_{,ah}$	47.65 ± 0.06	49.07 ± 0.45	50.18 ± 0.89	49.48 ± 0.87
$Kp_{,ha}$	-105.74 ± 0.19	-81.13 ± 2.12	-74.46 ± 11.64	-73.15 ± 10.04
$Kp_{,hh}$	364.04 ± 0.16	339.79 ± 1.24	334.14 ± 9.25	335.36 ± 8.71
$Kd_{,ha}$	19.93 ± 0.04	17.29 ± 0.31	16.15 ± 1.74	16.29 ± 1.44
$Kd_{,hh}$	23.44 ± 0.02	24.09 ± 0.20	24.50 ± 0.34	24.19 ± 0.33
$Ref_{,ankle}$	-0.0005 ± 0.00	0.0000 ± 0.00	0.0000 ± 0.00	0.0000 ± 0.00
$Ref_{,hip}$	-0.0052 ± 0.00	-0.0047 ± 0.00	-0.0046 ± 0.00	-0.0047 ± 0.00

References

Afschrift, M., Jonkers, I., De Schutter, J., De Groote, F., 2016. Mechanical effort predicts the selection of ankle over hip strategies in nonstepping

Table 3: Eigenvalue distribution of identified PD controllers

	DET	STO2	STO3	STO4
$Eig1$	-2.344 + 8.717i	-2.151 + 8.529i	-2.940 + 9.115i	-2.949 + 9.118i
$Eig2$	-2.344 -8.717i	-2.151 - 8.529i	-2.940 - 9.115i	-2.949 - 9.118i
$Eig3$	-0.987	-1.273	-0.181 + 0.046i	-0.181 + 0.046i
$Eig4$	0.715	1.032	-0.181 - 0.046i	-0.181 - 0.046i

Table 4: Eigenvalue distribution of identified FPD controllers

	DET	STO2	STO3	STO4
$Eig1$	-2.097 + 8.550i	-2.092 + 8.539i	-2.091 + 8.535i	-2.083 + 8.529i
$Eig2$	-2.097 - 8.550i	-2.092 - 8.539i	-2.091 - 8.535i	-2.083 - 8.529i
$Eig3$	-1.020	-0.991	-0.981	-0.967
$Eig4$	-0.053	-0.062	-0.061	-0.073

postural responses. Journal of neurophysiology 116, 1937–1945.

Boonstra, T.A., Schouten, A.C., Van der Kooij, H., 2013. Identification of the contribution of the ankle and hip joints to multi-segmental balance control. Journal of neuroengineering and rehabilitation 10, 23.

Center, O.S., 1987. Ohio supercomputer center. http://osc.edu/ark:/19495/f5s1ph73.

Engelhart, D., Boonstra, T.A., Aarts, R.G., Schouten, A.C., van der Kooij, H., 2016. Comparison of closed-loop system identification techniques to quantify multi-joint human balance control. Annual reviews in control 41, 58–70.

Goodworth, A.D., Peterka, R.J., 2018. Identifying mechanisms of stance control: a single stimulus multiple output model-fit approach. Journal of Neuroscience Methods 296, 44–56.

Hargraves, C.R., Paris, S.W., 1987. Direct trajectory optimization using nonlinear programming and collocation. Journal of Guidance, Control, and Dynamics 10, 338–342.

Horak, F.B., Nashner, L.M., 1986. Central programming of postural movements: adaptation to altered support-surface configurations. Journal of Neurophysiology 55, 1369–1381.

Jain, A.K., Mao, J., Mohiuddin, K., 1996. Artificial neural networks: A tutorial. Computer , 31–44.

Kelly, M., 2017. An introduction to trajectory optimization: how to do your own direct collocation. SIAM Review 59, 849–904.

Kiemel, T., Zhang, Y., Jeka, J.J., 2011. Identification of neural feedback for upright stance in humans: stabilization rather than sway minimization. Journal of Neuroscience 31, 15144–15153.

van der Kooij, H., van Asseldonk, E., van der Helm, F.C., 2005. Comparison of different methods to identify and quantify balance control. Journal of neuroscience methods 145, 175–203.

Kuo, A.D., 1995. An optimal control model for analyzing human postural balance. IEEE transactions on biomedical engineering 42, 87–101.

Moore, J., van den Bogert, A., 2015. Human standing controller parameter identification with direct collocation, in: 15th International Symposium on Computer Simulation in Biomechanics, ISB. pp. –.

Moore, J.K., van den Bogert, A.J., 2018. opty: Software for trajectory optimization and parameter identification using direct collocation. J. Open Source Software 3, 300.

Mordatch, I., Lowrey, K., Todorov, E., 2015. Ensemble-cio: Full-body dynamic motion planning that transfers to physical humanoids, in: Intelligent Robots and Systems (IROS), 2015 IEEE/RSJ International Conference on, IEEE. pp. 5307–5314.

Park, S., Horak, F.B., Kuo, A.D., 2004. Postural feedback responses scale with biomechanical constraints in human standing. Experimental brain research 154, 417–427.

Peng, X.B., Andrychowicz, M., Zaremba, W., Abbeel, P., 2018. Sim-to-real transfer of robotic control with dynamics randomization, in: 2018 IEEE International Conference on Robotics and Automation (ICRA), IEEE. pp. 1–8.

Peterka, R., 2002. Sensorimotor integration in human postural control. Journal of neurophysiology 88, 1097–1118.

Van Der Kooij, H., De Vlugt, E., 2007. Postural responses evoked by platform pertubations are dominated by continuous feedback. Journal of neurophysiology 98, 730–743.

Wächter, A., Biegler, L.T., 2006. On the implementation of an interior-point filter line-search algorithm for large-scale nonlinear programming. Mathematical Programming 106, 25–57. URL: https://doi.org/10.1007/s10107-004-0559-y, doi:10.1007/s10107-004-0559-y.

Welch, T.D., Ting, L.H., 2009. A feedback model explains the differential scaling of human postural responses to perturbation acceleration and velocity. Journal of Neurophysiology 101, 3294–3309.